On the optimization of generators for offshore direct drive wind turbines

Alasdair McDonald and Nurul Azim Bhuiyan

***Abstract*— The objective of this paper is to optimize direct drive permanent magnet synchronous generators for offshore direct drive wind turbines in order to reduce the cost of energy. A 6MW wind turbine design is assumed and parametric electromagnetic and structural generator models are introduced for a surface-mounted magnet generator topology (using magnets with high BH_{max}) and a flux-concentrating variant (using magnets with lower BH_{max}). These are optimized using a hybrid Genetic Algorithm and Pattern Search process and the results show that the surface-mounted permanent magnet generator produces the lower cost of energy. The choice of objective function is addressed and it is found that a simplified metric incorporating generator cost and losses proxy produces similar designs to a full cost of energy calculation. Further steps to improve the quality of the model include the effect of generator mass on the design and cost of the turbine tower and foundation, which can add €0.4m to the turbine cost. Further optimizations are carried out to show the impacts of magnetic material costs (doubling this leads to a €1.1/MWh increase in cost of energy) and generator diameter limits (increasing the upper limit from 6m to 8m leads to a 0.9% drop in cost of energy) have on the choice of optimum independent variables.**

***Index Terms*—Cost of energy, direct drive wind turbine, optimization, permanent magnet generator, structural model, tower and foundation.**

I. Introduction

A growing proportion of offshore wind turbine designs are now based on directly driven permanent magnet synchronous generators. Direct drive machines can offer higher reliability and reduced maintenance cost because of the omission of the gearbox from the drive train [1]. Some of the downsides of these generators include their large size (due to the high torque rating), requirements for large quantities of rare earth permanent magnets and the significant generator structures required to maintain the small air-gap clearance against the large attraction forces between the rotor and the stator [2]. The generator designer needs to deliver a number of performance characteristics including high efficiency, low power losses at part load, high availability, low machine mass, reduced volume and lower material and manufacturing costs. Normally the designers employ some element of optimization to achieve the best balance of these aspects [3].

The main purpose of this paper is to examine the process of optimizing large, low speed generators for offshore direct drive wind turbines, exploring the different objective functions that a machine designer could use. This is done for two different generator topologies to test whether the recommendation of objective functions is independent of the machine type. The paper also investigates the effect on the optimization of a number of factors that interest a typical designer: the inclusion of structural generator material in the objective function, the inclusion of the impact of generator mass on the cost of the turbine tower and foundation, the bounds of generator diameter and the sensitivity to magnet specific cost and turbine cost.

Different authors have approached the problem of formulating the objective function of such optimizations in different ways. Polinder shows an objective function that minimizes the cost of generator active materials (i.e. magnet, copper and iron) and the generator losses as well [4]. Polinder *et al.* show a comparison of different types of generator in terms of annual energy yield per cost, which is analogous to payback period [5]. Grauers optimized low speed permanent magnet machines using generator costs and losses, including an estimation of generator structural cost in [6]. The generator system cost is minimized in [7]. Amuhaya and Kamper discussed the importance of reducing the mass and cost of generator active materials [8]. Bazzo *et al.* outlined some objective functions to minimize costs and maximize efficiency which included minimizing active and structural materials cost and minimizing cost of losses to get maximum return of investment [9]. Zavvos *et al.* offered an analytical tool that minimizes the generators mass or cost by optimizing both the electromagnetic and structural design at the same time [10]. Wu *et al.* also outlined the optimization of generator rotor structure for minimum generator mass where deflections were constrained [11]. Others have looked at different optimization methods with different objectives. This study compares some of these different objective functions that can be used to produce generator designs for wind turbines and assesses their ability to produce a generator designs with low cost of energy.

There is a range of different optimization approaches that can be used by the designers to find the best value of an objective function from some set of available alternatives. Genetic Algorithms (GA) have been proved to be good and reliable methods of solving such problems. They are suitable for both constrained and unconstrained optimization problems. Although GAs are good at searching global optima over an entire problem region, the speed of convergence to the optimal point can be slow [12]. On the other hand, deterministic optimization methods like the pattern search (PS) are very efficient for local searching [13]. To compensate for the weaknesses of these two methods, a hybrid algorithm combining both methods was proposed in [14]. With this technique a global search is carried out first using the GA and an intermediate set of solutions are found after a few generations. These solutions are used as initial parameters for

A. McDonald and N. A. Bhuiyan are with the Institute of Energy and Environment, Department of Electronic and Electrical Engineering, University of Strathclyde, Glasgow G1 1XW, United Kingdom. (e-mail: alasdair.mcdonald@strath.ac.uk; nurul-azim-bhuiyan@strath.ac.uk).

the PS to run a local search. The solution from this Pattern Search is considered as the global optimal solution. In this paper the process is used in MATLAB [15] to optimize four different objective functions: (a) Torque per magnet mass, (b) Torque per generator active material cost, (c) the difference between generator active material costs and the wind turbine revenue for 5, 10 and 15 years period of operation and (d) the wind turbine cost of energy.

Most of the generator models in [4-11] focus on the active material and losses but do not consider the generator structure in detail. McDonald showed that the structural mass of a 5 MW permanent magnet direct drive generator can be more than 80% of its total mass [16]. Structures are designed by using radial, axial and tangential deflection models. The generator mass, which is part of turbine top head mass can affect the tower and foundation cost that goes into turbine capital cost and effect on cost of energy [17]. According to a NREL technical report, the substructure and foundation cost is 9% of the total offshore wind turbine cost [18]. It is a significant part of the total turbine cost. In this paper, models and results include generator active and structural materials, losses and annual energy production and the effect of generator mass on turbine tower and foundations.

In order to demonstrate the optimization process, two different generator rotor designs – using different magnet materials – are used and compared for a typical 6MW offshore wind turbine. This paper builds on the work of Eriksson and Bernhoff [19] and one generator uses surface-mounted Nd-Fe-B magnets and another uses ferrite magnets in a flux-concentrating arrangement. These are designed parametrically using lumped parameter models and equivalent circuits.

As well as investigating the effectiveness of different objective functions and comparing different generator types, this paper explores the effect of maximum allowable diameter on the optimal results. Sensitivity analyses are carried out by varying magnet costs and the cost of the rest of the turbine.

TABLE I
CHARACTERISTICS OF THE WIND TURBINE AND SITE WIND RESOURCES

Rated grid power (MW)	6
Rotor diameter (m)	145
Rated wind speed (m/s)	11
Cut in wind speed (m/s)	3
Cut out wind speed (m/s)	25
Rated rotational speed (rpm)	12
Optimal tip speed ratio	8.3
Coefficient of performance at optimal tip speed ratio	0.48
Wind turbine availability (%) [20]	94
Turbine capital cost (exc. generator and foundation) (k€)	17530
Site wind speed shape parameter	2.3
Site wind speed scale parameter (m/s)	10.8
Mean wind speed (m/s)	9.6

II. METHODOLOGY

The wind turbine in this case study is described at the beginning of this section. After that, the electromagnetic models of the generators are outlined, these lead to generator material characteristics, terminal voltage and inductance calculations. The explanation of generator structure, tower and foundation costs come after that. Next, the optimization process, independent variables, constraints, objective functions and post processing are described. Subsequent to that, further investigations including optimizations for the surface-mounted Nd-Fe-B generators and the flux-concentrating ferrite generators with different objective functions, with varied diameter constraints, the effect of structural materials of generator mass and that of generator mass on turbine structures and sensitivity analysis are defined.

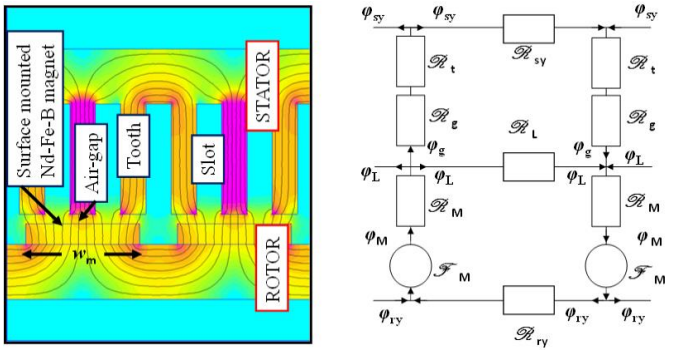

Fig. 1. (a) Magnetostatic finite element analysis of surface-mounted Nd-Fe-B generator, (b) Magnetic circuit. ■0T→■1.5T . Software is FEMM [21]

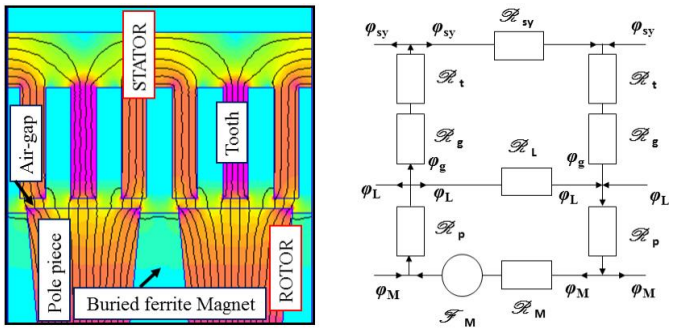

Fig. 2. (a) Magnetostatic finite element analysis of flux-concentrating ferrite generator, (b) Magnetic circuit. ■0T→■1.5T . Software is FEMM [21]

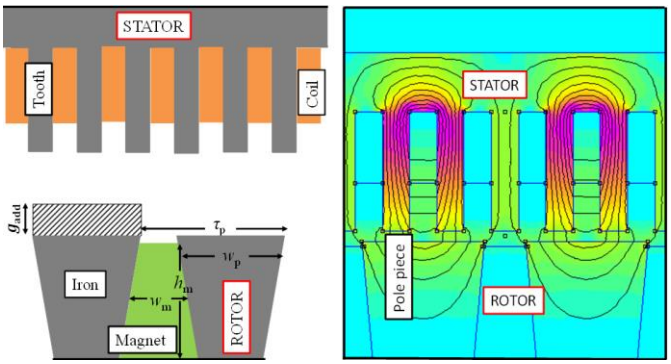

Fig. 3. Flux-concentrating ferrite magnet generator (a) additional air-gap height used in direct axis magnetizing inductance formulation (b) stator field lines in the quadrature axis

A. Turbine

A 6MW variable speed, 3 bladed, pitch regulated wind turbine is used in this study for offshore operation. It is assumed that the turbine rotor operates at its maximum power coefficient below the rated wind speed and hence has a rotational speed that varies in proportion to the wind speed. Once the turbine reaches the rated wind speed and power, the blades are pitched and the rotor speed is limited. The major ratings and assumptions are given in Table I. The probability of the wind speed being a certain value can be expressed by a Weibull distribution with shape and scale parameters given in Table I.

The site has a mean wind speed of 9.6m/s which is typical of some of the offshore wind farms planned for the North Sea.

B. Electromagnetic Model

The generators are modeled analytically in the steady state. The magnetic properties of the chosen magnet materials are given in [19]. Lumped parameter magnetic circuit models are used to calculate flux per pole. Simplified (linearized) sections of the two generator types with magnetic field and magnetic circuit models for one pole pair are shown in Fig. 1 and Fig. 2. The results from analytical model are verified using finite element software [21]. Flux density in the various parts of the system and the induced emf are calculated by using the results from these magnetic circuits as shown in [22].

It is assumed that the generators in this study run at unity power factor at all wind speeds. This simplification is applied to both generator types and reduces the complexity of the optimization. This assumption tends to overestimate the generator losses and material costs and underestimate the power converter rating and cost than for example varying the load angle so that the phase current is between the induced emf and terminal voltage [5].

In the case of a machine having PM mounted on the rotor surface, the direct axis and quadrature axis inductance are equal $L_\mathrm{d} = L_\mathrm{q}$ and hence $X_\mathrm{d} = X_\mathrm{q}$. The current, I is varied with wind speed hence the load angle, δ also varies to produce correct power. At higher wind speeds the induced emf, E increases up until the point that rotational speed becomes constant. Neglecting the voltage drop across the winding resistance, the terminal voltage is given by [23]

$$V = \sqrt{E^2 - (IX)^2} = E\cos\delta \tag{1}$$

where X is the reactance.

The generator with flux-concentrating ferrite magnet is a type of salient-pole machine and has different inductance in the direct and quadrature axis, i.e. $L_\mathrm{d} \neq L_\mathrm{q}$. The terminal voltage is given in [23],

$$V = E\cos\delta - I_\mathrm{d}\left(X_\mathrm{d} - X_\mathrm{q}\right)\cos\delta \tag{2}$$

where I_d is direct axis current. This can be solved to find the load angle for every wind speed if the relationships between wind speed and rotor speed and between wind speed and current are known. The magnetizing inductance can be calculated as given in [24],

$$L_\mathrm{m} = \frac{4\mu_0\tau_\mathrm{p} l_\mathrm{s}(k_\mathrm{w}N_\mathrm{s})^2}{p g_\mathrm{eff}\pi^2} \tag{3}$$

where μ_0 is the permeability of air, τ_p is the pole pitch, l_s is the stack length in axial direction. N_s is the number of turns of the phase winding, k_w is the winding factor, p is the number of pole pairs and the effective air-gap is $g_\mathrm{eff} = k_\mathrm{c} g$ where k_c is the Carter factor of the stator slot and g is the mechanical air-gap.

Direct axis and quadrature axis inductance can be calculated from the magnetizing inductance where effective air-gap is different. The effective air-gap in the direct axis, $g_\mathrm{eff,d}$ can be found by adding an additional air-gap g_add shown in Fig. 3(a), where the magnet reluctance $\mathscr{R}_\mathrm{m}$ is expressed in terms of air-gap reluctance.

$$\mathscr{R}_\mathrm{m} = \frac{w_\mathrm{m}}{\mu_0\mu_\mathrm{r,m}h_\mathrm{m}l_\mathrm{s}} = \frac{g_\mathrm{add}}{\mu_0\tau_\mathrm{p}l_\mathrm{s}} \tag{4}$$

$$g_\mathrm{add} = \frac{w_\mathrm{m}\tau_\mathrm{p}}{h_\mathrm{m}\mu_\mathrm{r,m}} \tag{5}$$

$$g_\mathrm{eff,d} = g_\mathrm{eff} + g_\mathrm{add} \tag{6}$$

where w_m is the width of magnet, h_m is the height of magnet and $\mu_\mathrm{r,m}$ is the relative permeability of ferrite magnet. For the quadrature axis, the majority of the flux found by using finite element software crosses only pole as shown in Fig. 3(b). The magnetic pole resembles a tooth surrounded by slots, and so the Carter factor can be applied to calculate the effective air-gap,

$$g_\mathrm{eff,q} = k_\mathrm{c,q} g_\mathrm{eff} \tag{7}$$

where $k_\mathrm{c,q}$ is the Carter factor from the rotor side in the quadrature axis,

$$k_\mathrm{c,q} = \frac{\tau_\mathrm{p}}{\tau_\mathrm{p} - g\gamma_\mathrm{q}} \tag{8}$$

$$\gamma_\mathrm{q} = \frac{4}{\pi}\left(\frac{w_\mathrm{m}}{2g}\arctan\left(\frac{w_\mathrm{m}}{2g}\right) - \ln\sqrt{1+\left(\frac{w_\mathrm{m}}{2g}\right)^2}\right) \tag{9}$$

The direct axis and quadrature axis inductances can be found as

$$L_\mathrm{d} = L_\mathrm{m,d} + L_\mathrm{m,u} + L_\mathrm{leakage} \tag{10}$$

$$L_\mathrm{q} = L_\mathrm{m,q} + L_\mathrm{m,u} + L_\mathrm{leakage} \tag{11}$$

where $L_\mathrm{m,d}$ is the d-axis magnetizing inductance, $L_\mathrm{m,q}$ is the q-axis magnetizing inductance, $L_\mathrm{m,u}$ is the mutual inductance which is one-third of the magnetizing inductance and L_leakage is the leakage inductance which can be calculated as [24].

The analytical results of direct axis and quadrature axis inductance are verified using finite element software which shows agreement within about 1% difference in both axes. Table II shows some key dependent variables verified using a 2D finite element software (FEMM) for the baseline generator design. In the case of the inductance calculations the 2D results do not include the end winding leakage inductance – these are calculated analytically. For the sake of comparison the analytical results presented in Table II also exclude the end winding leakage inductances.

TABLE II
ANALYTICAL RESULTS VS FEMM ANALYSIS RESULTS

Variables	Nd-Fe-B gen.		Ferrite gen.	
	Analytical	FEMM	Analytical	FEMM
Fundamental air-gap flux density, B_g (T)	1.00	0.99	0.98	0.97
Direct axis inductance, L_d (mH)	18.4	18.2	23.4	23.7
Quadrature axis inductance, L_q(mH)	18.4	18.2	25.9	26.2

Masses of different materials are calculated and translated into costs using data in Table III. In terms of the assumed costs, the turbine capital cost in Table I is calculated from [27]. Lamination cost and copper costs are taken from [5]. Permanent magnet, ferrite magnet, rotor iron, aluminum and structural steel cost including marginal cost increases in going from raw material costs to manufacturing costs is drawn from the authors' experience.

The influence of varying losses and generated power at each wind speed and annual energy production are calculated as shown in [5] and [22]. Reference [22] examined the influence of generator rotor inertia on the ability of wind turbines to

extract energy. That study found that even when the generator rotor inertia is doubled, the change in energy capture is extremely modest. This is probably due to the fact that the drivetrain inertia is 2 orders of magnitude smaller than the wind turbine rotor.

TABLE III
GENERATOR MATERIALS AND COST MODELING [5]

Generator Material Characteristics	
Slot filling factor	0.6
Resistivity of copper at 120ºC (μΩ·m)	0.024
Eddy-current losses in laminations at 1.5 T, 50 Hz (W/kg)	0.5
Hysteresis losses in laminations at 1.5 T, 50 Hz (W/kg)	2
Cost Modeling	
Lamination cost (€/kg)	3
Copper cost (€/kg)	15
Permanent magnet cost (€/kg)	60
Ferrite magnet cost (€/kg)	3
Rotor iron cost (€/kg)	2
Aluminum cost (€/kg)	10
Structural steel cost (€/kg)	2
Price of kWh energy (€/kWh)	0.19

C. Generator Structural Model

In order to design lightweight and cost effective direct drive generators, the designer should include a structural model of the generator along with the active material model. McDonald [16] showed the structural models with different types of rotor and stator structures for direct drive generators. In this study a simple structure – where a cylinder is connected to the shaft by arms – has been used to represent both the generator rotor and stator. An example rotor and stator structure and different types of deflection with 6 arms is shown in Fig. 4 and Fig. 5. The cylinder includes the 'yoke' or back iron. For the flux-concentrating ferrite generator there is no steel rotor yoke; instead of steel, pole pieces are mounted on an aluminum cylinder. During the optimization process the rotor deflection is allowed to deflect radially into air-gap by 5% of the air-gap length, the tangential deflection is 0.5% of the air-gap and the structure is allowed to deflect axially by 0.02% of the air-gap. The maximum allowed diameter used for optimization is the same for both generators. The mechanical air-gap is kept as a fixed proportion of the air-gap diameter D, so that $g = D / 1000$. As the radial height of the flux-concentrating poles is larger than that of a surface-mounted magnet, the rotor structure is slightly larger when using the surface-mounted Nd-Fe-B magnets.

The electromagnetic and structural models are linked and so if the air-gap flux density increases then the loads on the rotor and stator increase. This means that if the magnet MMF increases or if the air-gap clearance is reduced (and the air-gap reluctance drops) then the loading increases. In order to keep the air-gap open, stiffer and heavier generator structures are needed.

A mean normal radial stress, q_r is applied to the outside surface of the rotor leads to a radial deflection,

$$q_r = \frac{{B_g}^2}{2\mu_0}\frac{w}{\tau_p} \tag{12}$$

where B_g is the air-gap flux density, $w = w_m$ for surface-mounted Nd-Fe-B generator and $w = w_p$ for flux-concentrating ferrite generator. In this paper, the structural dimensions of the arms and yoke are varied to meet the deflection criteria. In the flux-concentrating ferrite generator case, additional aluminum cylinder thickness is added. Equation (12) shows that the loads on the structure are strongly dependent on the electromagnetic model.

The radial deflection at the mid-point between two arms is given in [1] and [16] as,

$$u = \frac{q_r R^2}{Y h_y}\left(1 + \frac{R^3}{I_r}\alpha\right) \tag{13}$$

where R is the outer radius of the structure, Y is the Young's Modulus of the structural material, h_y is the height of yoke, I_r is the second moment of area of the cross-section of yoke and α is a function of the number of arms and the dimensions of the rotor structure [25].

In terms of the tangential direction, the deflection z for the rotor or stator structure can be found as [25],

$$z = \frac{T_{max} {l_{ar}}^3}{12 Y I_z} \tag{14}$$

where T_{max} is the maximum torque of generator, l_{ar} is the radial length of the arms and I_z is the second moment of area of the structural arms in the circumferential direction.

The axial deflection of the generator rotor or stator due to gravity, y is given in [16] and [25] as

$$y = \frac{W {l_b}^3}{12 Y I_y} + \frac{w {l_{ar}}^4}{24 Y I_y} \tag{15}$$

where W is the weight component of the back iron (i.e. permanent magnet, copper, aluminum, iron or other materials in rotor or stator yoke), l_b is the radial length of the beam, w is the weight component of the arms and I_y is the second moment of area of the structural arms in the axial direction.

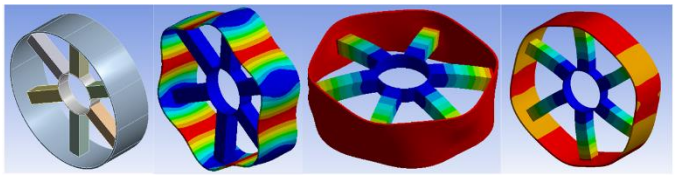

Fig. 4. From left to right, (a) Structural model of rotor (b) Radial deflection (c) Axial deflection (d) Tangential deflection

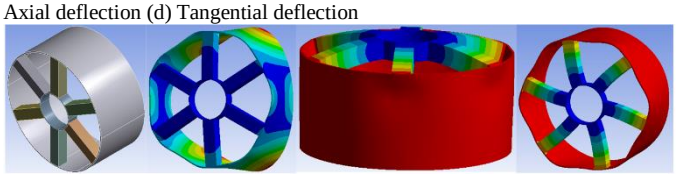

Fig. 5. From left to right, (a) Structural model of stator (b) Radial deflection (c) Axial deflection (d) Tangential deflection

The structural mass of generator can be found by the summation of the structural mass of rotor and the structural mass of stator found after optimization. The structural mass of rotor or stator, m_{str} can be calculated as

$$m_{str} = \rho\left[2\pi R h_{y0} l_s + n_{ar} l_{ar}\{bd - (b - 2t_a)(d - 2t_a)\}\right] \tag{16}$$

where ρ is the density of the material, R is the outer radius of the structure, h_{y0} is the extra yoke height due to deflection, n_{ar} is the number of arms, b is the average beam width (circumferential), d is the average beam width (axial) and t_a is the wall thickness of beam.

D. Tower and Foundation cost

Although heavily influenced by the height of the tower and the swept area of the wind turbine rotor, the tower mass, m_{tower}

also depends on the top head mass (the combined mass of the wind turbine rotor and the equipment in the nacelle, including the generator). This top head mass can be calculated as,

$$m_{\mathrm{top}} = m_{\mathrm{rtop}} + m_{\mathrm{act}} + m_{\mathrm{str}} \quad (17)$$

where m_{rtop} is the rest of the turbine top head mass excluding the generator mass m_{act} is the generator active material mass and m_{str} is the generator structural mass. The rest of the turbine top head mass is based on [26].

To investigate the effect of increased top head mass on the tower mass, a relationship between tower mass and top head mass (for a 90m hub height) can be found by fitting a power law curve to the data in [26],

$$m_{\mathrm{tower}} = 2.84 {m_{\mathrm{top}}}^{0.943} \quad (18)$$

Using the structural steel cost from Table III, the tower cost's relationship to top head mass, C_{tower} (k€) can be approximated by a linear function in the range $400 < m_{\mathrm{top}} < 600$ tonnes as,

$$C_{\mathrm{tower}} = 0.0025 m_{\mathrm{top}} + 75.3 \quad (19)$$

In terms of foundation type, a monopile was assumed in this study. Based on [27] and [28], for a 6MW wind turbine with a 90m hub height in 30m water depth, the relationship of substructure and foundation mass, m_{sf} with top head mass can be given as

$$m_{\mathrm{sf}} = 1137 \times 10^3 + \frac{{m_{\mathrm{top}}}^{1.13}}{10} \quad (20)$$

Using the steel cost from Table III (assuming 60% pile and 40% transition piece and outfitting steel), The effect of any increased generator mass on the turbine substructure and foundation cost, C_{sf} (k€) can be approximated by a linear function for $400 < m_{\mathrm{top}} < 600$ tonnes as,

$$C_{\mathrm{sf}} = 0.0015 m_{\mathrm{top}} + 2644.1 \quad (21)$$

E. Optimization

Design optimization methods generally use an algorithm which take independent variables as input and vary those input to evaluate dependent variables in machine model and hence optimize an objective function (subject to predetermined constraints). In this paper, the independent variables and constraints are described in the following subsection 1. The analytical models are used to evaluate a range of different dependent variables, some of them contribute to the objective functions laid out in subsection 2. The process is driven by an optimization algorithm as described in subsection 3.

1) Independent Variables and Constraints

Independent variables used in this study are machine diameter, axial length, magnet height, the ratio of magnet width to pole pitch, number of pole pairs and tooth height. The lower boundaries (LB) and the upper boundaries (UB) of independent variables for both generators are given in Table IV.

To simplify the optimization, a number of assumptions and constraints are used, such as setting the air gap clearance to a fixed ratio of the machine diameter, maximum flux density to avoid saturation in stator and rotor yoke and limiting rated electrical power to greater than or equal to 6 MW.

TABLE IV
BOUNDARY LIMITS FOR INDEPENDENT VARIABLES

Independent Variables	Nd-Fe-B gen.		Ferrite gen.	
	LB	UB	LB	UB
Air gap diameter, D (m)	6	10	6	10
Axial length, l_s (m)	0.7	1.8	0.7	1.8
Magnet width/pole pitch, w_m/τ_p	0.5	0.9	0.6	0.9
Magnet height, h_m (m)	0.01	0.04	0.1	0.45
Pole pairs, p (-)	60	100	60	100
Height of tooth, h_t (m)	0.04	0.09	0.04	0.09

2) Objective Functions

Four different objective functions are used in this study. According to the aim of minimizing the use of Nd-Fe-B magnets, the first objective function is rated generator torque T per magnet mass m_{PM}. This tries to minimize the amount of magnet material. In this case the objective function is,

$$F_1 = \frac{T}{m_{\mathrm{PM}}} \quad (22)$$

The second objective function, F_2 seeks to minimize the cost of the electromagnetically active materials instead of only considering the magnet mass. The active materials cost includes the magnet cost C_{pm}, copper cost C_{Cu} and active iron cost C_{Fe}. This objective function is

$$F_2 = \frac{T}{C_{\mathrm{PM}} + C_{\mathrm{Cu}} + C_{\mathrm{Fe}}} \quad (23)$$

The third objective function, F_3, presented in [4] seeks to minimize the cost of active material while maximizing the revenue produced from the wind turbine over a number of years, P_y. In this paper this objective function is assessed with P_y = 5, 10 and 15 years. This time period is multiplied by C_E, the revenue corresponding to 1 kWh of electrical energy and E_y, the annual energy yield of the turbine,

$$F_3 = C_{\mathrm{PM}} + C_{\mathrm{Cu}} + C_{\mathrm{Fe}} - P_y C_E E_y \quad (24)$$

The ultimate customer of the wind turbine manufacturer wants the lowest cost of energy and so the final objective function calculates this [18],

$$F_4 = \frac{(FCR \times ICC) + AOM}{E_y} \quad (25)$$

where *FCR* is the fixed charge rate, *ICC* is the initial capital cost of the turbine (including the generator), *AOM* is the annual operation and maintenance (assumed to be unaffected by the generator design). The variation of the independent variables lead to changes in capital cost and energy yield.

3) Optimization Process

A hybrid Genetic and Pattern Search algorithm which has been developed in MATLAB is used here as an optimization procedure [29]. A GA can reach the region near an optimum point relatively quickly but it takes longer to achieve convergence. A commonly used technique is to run the GA for a small number of generations to get near to an optimum point. Then the solution from the GA is used as an initial point for another optimization solver that is faster and more efficient for a local search. In this case, the GA developed by [15] was used. GA choose the initial input randomly from the ranges of independent variables. The hybrid optimization algorithm [29] runs in a way that takes the results of the Genetic Algorithm as an initial guess for the Pattern Search to get the global minimum for each of the objective functions.

Fig. 6 shows the flow chart of the optimization process. The Genetic Algorithm starts by generating an initial population randomly from the boundary limit design space of independent variables given in Table IV. For this initial population, the GA evaluates the fitness of each candidate against a given objective function. The GA runs for a number of generations (until it reaches the maximum generation number set for this algorithm) and in each generation, a new population is created using selection, crossover and mutation. The best results after the maximum generations of GA (which are near to the global optimal result) are used as the initial point of the Pattern Search algorithm (PS) to make a further optimization (local search near to global optimal point). At the next step, the PS constructs a pattern vector to create mesh point using the results of independent variables from the GA. After that, the PS evaluates the fitness of this initial mesh point for the given objective function. If there any improved results found at the mesh point, then the PS expands the mesh size and constructs a new pattern vector to create a new mesh point and evaluates the fitness of the new mesh point. If there is no improvement in results and no stopping criteria occurs, then the PS contracts the mesh size and evaluates the fitness of the new mesh point. If any stopping criteria occur then the PS gives the final result of optimization. Stopping criteria includes constraint, function and mesh tolerance.

The number of generation used for the GA is 4 (after 4 generations the GA gives results near to the global optimal solution in this study), the population size is 100, the maximum stall generation is 10 and the function tolerance is 1×10^{-3}. The mutation function chosen is adaptive feasible. For the Pattern Search algorithm, the mesh size expansion factor is 2 and the mesh size contraction factor is 0.5 [29].

A typical optimization run for a surface mounted Nd-Fe-B generator takes 7 min in MATLAB 2014 on a 64 bit Windows 7 operating system on a PC with an Intel core i7 3.4GHz processor.

4) Post Processing

After the optimization process is complete, the equation (22) to (25) are applied to all the optimized designs to compare the results of objective functions in each optimized design. Dependent variables such as efficiency, annual energy production, losses, flux density, cost and masses of different active and structural materials are produced after optimization.

F. Runs/Investigations

Initially the optimization program was run for surface-mounted Nd-Fe-B and flux-concentrating ferrite generators for each of the four objective functions. After this the maximum allowed diameter constraint was varied from 6m to 16m in steps and the 3rd objective function was used in the optimization process.

The optimization program was run with both fixed and variable generator structural materials to see the effect on the cost of energy. For the fixed generator structural materials, a fixed cost is included with turbine initial capital cost and the structural mass also fixed. For the variable generator structural materials, when the generator dimensions varies, structural mass is calculated and cost also varies. The effect of varying the top head mass is included in some runs, with the outputs compared to runs which do not include variation in these elements. Finally, a sensitivity analysis was performed on the magnet price and rest of the turbine cost to see the effect on the cost of energy.

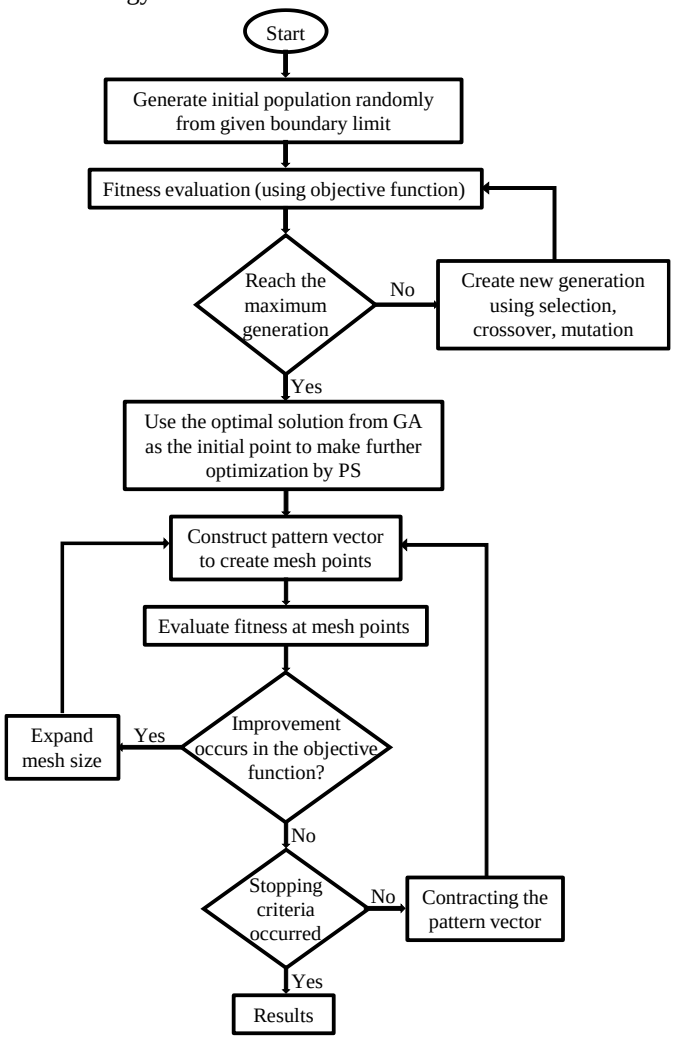

Fig. 6. Flow chart for optimization process

III. Results

A. Surface-mounted Nd-Fe-B Generator

Table V shows the independent variables selected by the optimization for the objective functions (where F_3(i), F_3(ii), F_3(iii) represents the third objective function when P_y is 5, 10 and 15 years respectively). Fig. 7 shows the efficiency curves for these different designs with surface-mounted Nd-Fe-B magnet and Fig. 8 shows the post-processed optimization results using (22)-(25).

TABLE V

Independent Variables vs Objective Functions; Nd-Fe-B

Independent variables	F_1	F_2	F_3(i)	F_3(ii)	F_3(iii)	F_4
Air gap diameter, D (m)	9.03	8.36	9.99	9.99	9.99	9.92
Axial length, l_s (m)	1.62	1.17	1.19	1.33	1.41	1.17
Magnet width/pole pitch, w_m/τ_p	0.69	0.81	0.8	0.82	0.82	0.81
Magnet height, h_m (m)	0.012	0.018	0.021	0.023	0.025	0.021
Pole pairs, p (-)	100	100	98	79	72	100

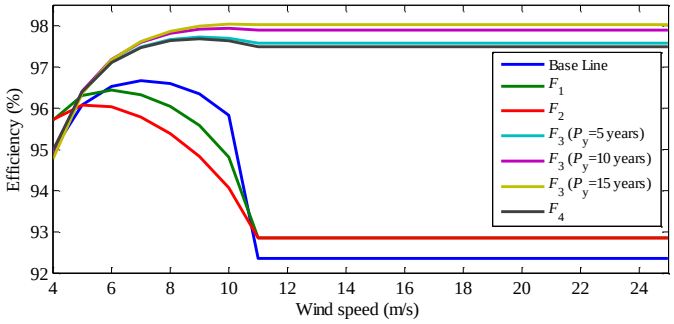

Fig. 7. Baseline and optimized efficiency curves for different objective functions with surface-mounted Nd-Fe-B generators

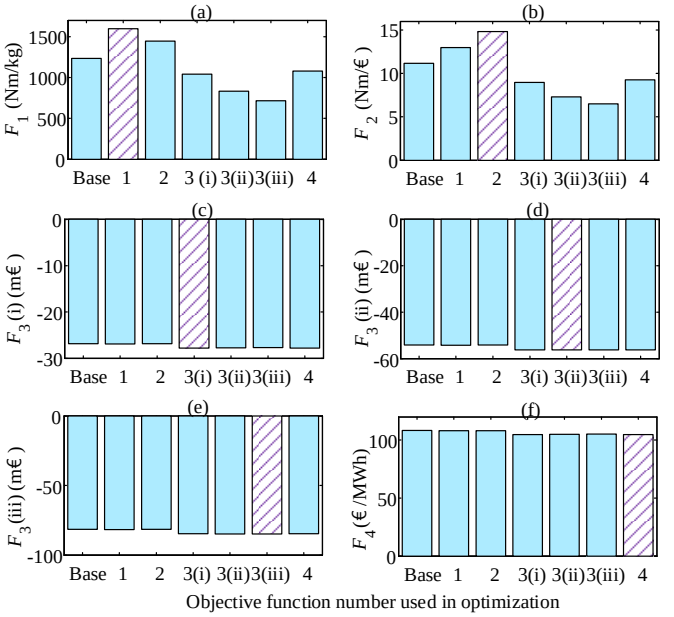

Fig. 8. Optimization results of different objective function for the surface-mounted Nd-Fe-B generators

The objective function F_3 (with P_y=15 years) gives the highest efficiency at rated wind speed which is 98.0% and except the baseline, F_1 and F_2 give the lowest efficiency of 92.9%. F_3 and F_4 give similar efficiency at rated wind speed where F_3 is slightly higher than F_4; efficiency in F_3 increases with P_y.

The *y*-axis of Fig. 8(a) shows the evaluated results of F_1 – equation (22) – for each of the different objective functions (as displayed on the *x*-axis) after post-processing. Similarly Figs. 8(b)-(f) show the results for F_2-F_4. Each sub-figure has the optimal result highlighted, these values are 1598.4 Nm/kg, 14.8 Nm/€, -€27790k, -€56314k, -€84892k and €104.8/MWh.

B. *Flux-concentrating Ferrite Generator*

Table VI shows the independent variables selected by the objective functions for the flux-concentrating ferrite machine. Fig. 9 shows the optimization results for the different objective functions after post-processing.

The flux-concentrating ferrite magnet generators have similar efficiency to the Nd-Fe-B machines: F_3 gives maximum efficiency 97.8% at rated wind speed and F_1 and F_2 give a lower efficiency of 92.9%. F_3 and F_4 give similar efficiency where F_3 is slightly higher.

Fig. 9 is laid out as Fig. 8 is, with the evaluated results of F_1–F_4 for each of the different objective functions after post-processing. In each sub-figure the optimal result is highlighted, i.e. 140.8 Nm/kg, 13.6 Nm/€, -€27636k, -€56112k, -€84623k and €105.8/MWh.

C. *Impact of Generator Air-gap Diameter Constraints*

Fig. 10 shows the impact of the choice of upper limit of the generator air-gap diameter for both surface-mounted Nd-Fe-B generator and flux-concentrating ferrite generator. By varying the maximum allowed boundary for both generators diameter from 6m to 16m, it can be seen that the optimal value for the surface-mounted Nd-Fe-B generator is near to 11.7m and for the flux-concentrating ferrite generator, it is 12.6m. The cost of energy in surface-mounted Nd-Fe-B generator varies from €106.2/MWh to €105.2/MWh and the cost of energy in flux-concentrating ferrite magnet generator varies from €107.1/MWh to €106.2/MWh. The largest drop in cost of energy occurs when extending the upper limit from 6m to 8m.

The total generator mass for the surface-mounted Nd-Fe-B generator varies from 75.6 tonnes to 105.5 tonnes and from 215.1 tonnes to 231.3 tonnes for the flux-concentrating ferrite machine. To allow smooth optimization, the maximum allowable magnet height is flexible for the flux-concentrating ferrite generator with 6m and 8m air-gap diameter. This leads to the largest active material mass in the 8m air-gap diameter generator.

D. *Effect of Generator and Turbine Structural Models*

When the generator structural model are included in the optimization process (using the F_4 objective function to optimize the surface-mounted Nd-Fe-B generator) then the deflections are 0.5mm in the radial direction, 0.43mm in the tangential direction and 0.23mm in the axial direction. Similar results are found for the flux-concentrating machines. The cost of energy increased by 0.26% in surface-mounted Nd-Fe-B generator and by 0.29% in flux-concentrating ferrite magnet generator when the structural model and its limits are included.

If the radial deflection limit for the surface-mounted Nd-Fe-B generators is relaxed from 5% to 7% and 10% of the air-gap clearance, the optimal fundamental air-gap flux density increases from 0.92T to 0.95T and 0.97T and the optimal air-gap diameter decreases from 9.92m to 9.83m and 9.8m respectively.

When the turbine structural model is included then the tower cost increased by €2.54k for the addition of one tonne of generator mass; this is about 0.012% of the total wind turbine cost. The offshore substructure and foundation cost increased by €1.5k for every additional one tonne of generator mass, which is about 0.007% of the total wind turbine cost.

TABLE VI
INDEPENDENT VARIABLES VS OBJECTIVE FUNCTIONS; FERRITE

Independent variables	F_1	F_2	F_3(i)	F_3(ii)	F_3(iii)	F_4
Air gap diameter, D (m)	9.24	9.14	9.99	9.99	9.99	9.9
Axial length, l_s (m)	1.64	1.51	1.45	1.48	1.63	1.29
Magnet width/pole pitch, w_m/τ_p	0.69	0.6	0.75	0.76	0.82	0.78
Magnet height, h_m (m)	0.23	0.28	0.38	0.45	0.45	0.39
Pole pairs, p (-)	88	100	73	64	60	74

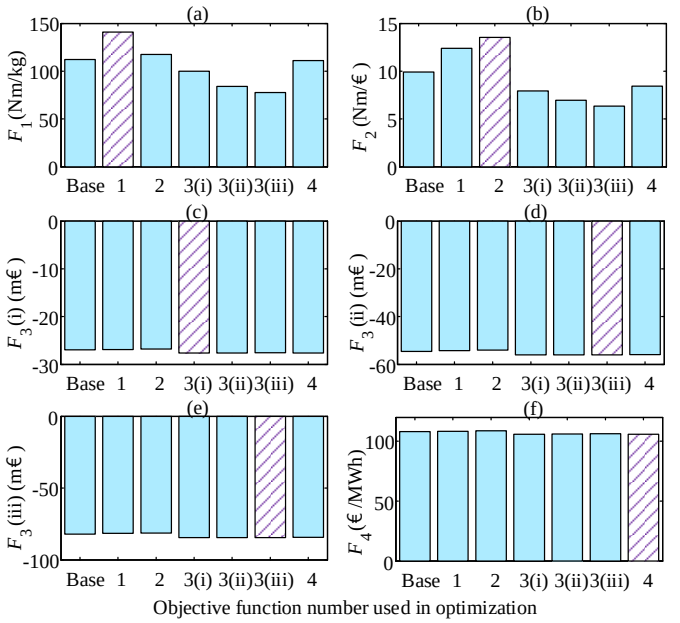

Fig. 9. Optimization results of different objective function for the flux-concentrating ferrite generators

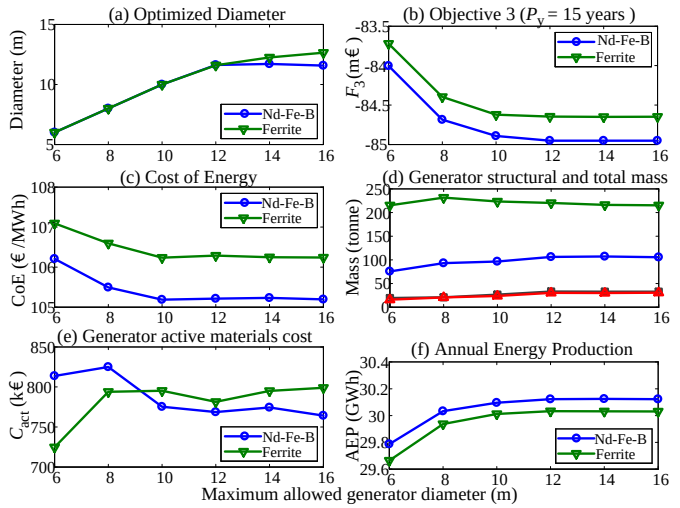

Fig. 10. Impact of the choice of maximum allowed generator air-gap diameter. In subfigure (d), the following series are represented accordingly: (■) Nd-Fe-B structural mass, (○) Nd-Fe-B total mass, (△) Ferrite structural mass, (▽) Ferrite total mass

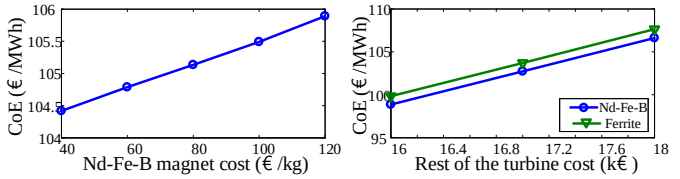

Fig. 11. Sensitivity of cost of energy for different variables. (a) Cost of a kg of Nd-Fe-B (b) Cost of the rest of the turbine.

E. Sensitivity to Magnet and Rest of Turbine Cost

Fig. 11 shows the sensitivity of the cost of energy for different magnet costs and the cost of the rest of the turbine had been assumed to be constant in the optimization process. Fig. 11(a) shows that if the Nd-Fe-B cost increases to €120/kg, the cost of energy would rise to €105.9/MWh. However, if the magnet costs fall to €40/kg, the cost of energy will fall back to €104.4/MWh. If the rest of the turbine cost varies from €16m to €18m as shown in Fig. 11(b), the difference in cost of energy between the two types of generators remains constant.

IV. Discussions

A. On the Choice of Objective Function

It can be seen that the objective functions F_3 and F_4 produce higher efficiency designs for both types of generators than the objective functions F_1 and F_2. This is unsurprising as the formulation for F_3 and F_4 explicitly includes annual energy yield. The major difference in losses between F_1 & F_2 and F_3 & F_4 is due to the copper losses. Higher current density is used to increase electrical loading in F_1 & F_2, which implies higher copper losses. For F_1 this allows reduced magnetic loading and hence a reduction in magnet mass; for F_2 the higher electrical loading leads to a reduction in both magnet and copper mass. The balance of copper and iron losses are slightly different with F_3 & F_4 having slightly higher iron losses. In machine design it is often the case that lower losses are found when contributions from copper and iron losses are more closely balanced.

In terms of the application, a balance of high efficiency and low cost is attractive. The designs resulting from the 1st and 2nd objective functions give a high cost of energy when evaluated post-optimization. F_1 and F_2 reduce the volume of active material (magnet mass in the case of F_1 and all the active material, weighted by their specific costs in the case of F_2) for the rated torque at the expense of higher losses. Although their generator capital costs are lowest, they achieve this by sacrificing annual energy yield. In reality the generator capital cost is only a modest contributor to the total turbine capital cost and yet generator inefficiency affects all of the turbine power output. So the 1st and 2nd objective functions are a poor choice in terms of cost of energy for the optimization of wind turbine generators.

The optimized design parameters and the ultimate cost of energy are very similar for F_3 and F_4. Different turbine costs and parameters could lead to a larger difference between F_3 and F_4, however it appears that F_3 is quite a good proxy for F_4. The change in the number of years for F_3 makes a slight difference in the cost of energy. The higher the number of years used (i.e. 10 and 15 years rather than 5 years) produces more efficient designs, but also increases the cost of energy for this case study. For larger, more capitally expensive offshore wind turbines (e.g. those in deeper waters) it may be useful to opt for 10 or 15 years when using F_3. One of the benefits of the 3rd objective function is that it does not need detailed turbine information and so is more general in comparison to 4th objective function.

B. On the Choice of Generator Topology

The surface-mounted Nd-Fe-B generator topology gives marginally better cost of energy in comparison to the flux-concentrating ferrite magnet generator due to its higher efficiency and hence higher energy yield. The active material cost in the flux-concentrating ferrite magnet generators is slightly higher and the generator mass is higher because of a large difference in magnet mass and rotor iron mass (the mass of pole pieces exceeds that of the rotor yoke in the other machine). Torque per magnet mass in the surface-mounted Nd-Fe-B machine is unsurprisingly very high because of the magnet mass difference. The structural cost in

flux-concentrating ferrite magnet machines is higher (in most of the objective functions) while the structural masses are lower in comparison to surface-mounted Nd-Fe-B machines. This is because the flux-concentrating machine uses lightweight – but relatively expensive – aluminum in the rotor structure of flux-concentrating in order to avoid high permeability paths which can encourage leakage flux.

C. On the Impact of Air-gap Diameter Constraints

Constraining the diameter of the generator is often necessary for onshore wind turbines as there are limits to what can be transported by road; for offshore turbines this is not necessarily the case. Allowing the upper limit of diameter to increase to 10m reduces the turbine cost of energy by about 1%; further increases in air-gap diameter yields only small marginal gains and these are unlikely to be worth the extra effort involved in the manufacturing processes and cost of larger manufacturing tooling and facilities. The cost and mass of the generator structure increases with increasing the diameter for both generator types. In smaller diameter generators, the cost of generator active materials is slightly higher in the surface-mounted Nd-Fe-B generators. Annual energy production generated by lower diameter generators is slightly lower for both generator types.

D. On the Effect of Including Structural Materials

Including generator structural materials can affect the generator mass and hence the tower and foundation cost (described in subsection IV-E). It was found that when the generator structural materials were included in the optimization model, the cost of energy increased by 0.26% for the surface-mounted Nd-Fe-B generators and by 0.29% for the flux-concentrating ferrite magnet generators. While they have similar structural masses, the increase in cost of energy is higher for the ferrite magnet machine because aluminum – which is relatively expensive – is used in its rotor structure.

E. On the Impact of Generator Mass

The active material mass in the ferrite magnet generator is about 200% more than for the Nd-Fe-B generators. The additional rotational inertia (due to the extra mass on the generator rotor) does not make a significant change to the energy capture of the turbine. The mass difference of generator active materials between the Nd-Fe-B generator and ferrite generator in [22] is similar to the mass difference of optimized generators (for objective 4) in this paper (78 tonnes in [22] and 88 tonnes here). The change in annual energy capture with higher inertia was negligible in [22].

The increased top head mass – due to a heavier generator – can affect the tower costs and foundation costs. Typically the ferrite magnet generators are about 100 tonnes heavier (including structural mass), implying that the tower costs would be €254k more expensive and the substructure and foundation costs would be €150k more expensive than the equivalent Nd-Fe-B generator. These figures can be higher depending on the water depth.

F. On the Sensitivity to Specific Magnet Cost and Rest of Turbine Cost

If the specific cost of Nd-Fe-B magnets were to increase by a large enough margin (while the ferrite magnet material cost remained constant) then the flux-concentrating ferrite machine would become more attractive from a cost of energy perspective. However in this study even if the specific magnet cost doubled (from €60/kg to €120/kg) the cost of energy is still lower for the generator using Nd-Fe-B magnets than for the flux-concentrating ferrite machine. The cost of energy sensitivity to specific magnet cost might be more significant for onshore turbines, as the rest of the turbine has lower capital costs. However, when varying the rest of the turbine cost, the gap between the cost of energy for the two generators did not change significantly.

V. Conclusions

The results of a number of optimizations with different objective functions have been shown for offshore direct drive wind turbine generators. If ones ultimate aim is to reduce the cost of energy of a turbine through better generator design then F_3 and F_4 are good choices and F_1 and F_2 are rather poor objective functions. Despite being quicker to formulate and needing only limited information about the turbine, F_3 is a close proxy for F_4; the latter explicitly models the cost of energy and so it is able to find a marginally better cost of energy.

The investigation was carried out on two different machine topologies and the conclusion about objective functions is independent of the machine type. It has been shown that the minimum cost of energy of a flux-concentrating ferrite generator is about 0.93% higher than that of a surface-mounted Nd-Fe-B generator and the total generator mass (active and structural mass) is about 100% heavier. Even if the specific cost of Nd-Fe-B magnets were to double, the cost of energy is still lower than that of a flux-concentrating ferrite magnet generator.

It has also been demonstrated that it is important to include structural modelling and materials when optimizing direct drive wind turbine generators for three reasons: (a) it impacts on the generator cost estimation by more than 0.25%, (b) the added top head mass affects the tower and foundation costs estimation by about €0.4m and (c) it allows the maximum allowed diameter to be varied. In the latter case, the largest drop in cost of energy is when the air-gap diameter upper limit is increased from 6m to 8m. The drop in cost of energy is about 0.9% for both generator types.

VI. References

[1] A. S. McDonald, M.A. Mueller and H. Polinder, "Structural mass in direct-drive permanent magnet electrical generators," *IET Renew. Power Generation*, vol. 2, no. 1, pp. 3-15, Mar. 2008.

[2] M. A. Mueller, A. S. McDonald, D. E. Macpherson, "Structural analysis of low-speed axial-flux permanent-magnet machines," *IEE Proc. –Electr. Power Appl.*, vol. 152, no. 6, pp. 1417–1426, Nov. 2005.

[3] D. C. Aliprantis, S. D. Sudhoff and B. T. Kuhn, "Genetic algorithm-based parameter identification of a hysteretic brushless exciter model," *IEEE Trans. Energy Convers.*, vol. 21, no. 1, pp. 148-154, Mar. 2006.

[4] H. Polinder, "Principles of electrical design of permanent magnet generators for direct drive renewable energy systems," in *Electrical Drives for Direct Drive Renewable Energy Systems*, M. Mueller, H. Polinder, Ed. UK: Woodhead Publishing, 2013, ch. 2, pp. 43.

[5] H. Polinder, F. F. A. Van der Pijl, G. J. De Vilder, and P.J. Tavner, "Comparison of direct-drive and geared generator concepts for wind

turbines," *IEEE Trans. Energy Convers.*, vol. 21, no. 3, pp. 725-733, Sept. 2006.
[6] A. Grauers, "Design of direct-driven permanent-magnet generators for wind turbines," Ph.D. dissertation, Chalmers Univ. Technol., Goteborg, Sweden, 1996.
[7] H. Li, Z. Chen, and H. Polinder, "Optimization of multibrid permanent-magnet wind generator systems," *IEEE Trans. Energy Convers.*, vol. 24, no. 1, pp. 82–92, Mar. 2009.
[8] J. H. J. Potgieter and M. J. Kamper, "Optimum Design and Comparison of Slip Permanent-Magnet Couplings With Wind Energy as Case Study Application," *IEEE Trans. Ind. appl.*, vol. 50, no. 5, pp. 3223–3234, Sept. 2014.
[9] T. Bazzo, J. F. Kolzer, R. Carlson, F. Wurtz, and L. Gerbaud, "Optimum design of a high-efficiency direct-drive PMSG," in *2015 IEEE Energy Convers. Congr. and Exposition*, Montreal, QC, 2015, pp. 1856-1863.
[10] A. Zavvos, A. McDonald, and M. Mueller, "Optimisation tools for large permanent magnet generators for direct drive wind turbines," *IET Renew. Power Generation*, vol. 7, no. 2, pp. 163-171, Mar. 2013.
[11] Z. Y. Wu, R. H. Qu, J. Li, H. Y. Fang, and Z. S. Fu, "Structure optimization of rotor supporting of permanent magnet direct drive synchronous generators for large wind turbine based on genetic algorithm and finite element method," in *2015 IEEE Int. Elect. Mach. & Drives Conf.*, Coeur d'Alene, ID, 2015, pp. 1755-1760.
[12] K. Choi, D. H. Jang, S. I. Kang, J. H. Lee, T. K. Chung and H. S. Kim, "Hybrid Algorithm Combing Genetic Algorithm With Evolution Strategy for Antenna Design," *IEEE Trans. Magn.*, vol. 52, no. 3, pp. 1-4, Mar. 2016.
[13] J.-K. Kim, D.-H. Cho, H.-K. Jung, and C.-G. Le, "Niching genetic algorithm adopting restricted competition selection combined with pattern search method," *IEEE Trans. Magn.*, vol. 38, no. 2, pp. 1001–1004, Mar. 2002.
[14] Y. Tai, Z. Liu, H. Yu, and J. Liu, "Efficiency optimization of induction motors using genetic algorithm and Hybrid Genetic Algorithm," in *Proc. Int. Conf. Elect. Mach. and Syst.*, Beijing, China, 2011, pp. 1-4.
[15] A. Chipperfield, P. Fleming, H. Pohlheim, C. Fonseca, *Genetic Algorithm Toolbox for use with MATLAB.* (1994) [Online]. Available at: http://codem.group.shef.ac.uk/index.php/ga-toolbox
[16] A. McDonald, "Structural analysis of low speed, high torque electrical generators for direct-drive renewable energy converters," Ph.D. dissertation, Dept. Eng. And Electron., Univ. Edinburgh, Edinburgh, Scotland, 2008.
[17] L. Fingersh, M. Hand, A. Laxson, "Wind turbine design cost and scaling model," Nat. Renew. Energy Lab., Golden, CO, USA, Tech. Rep. NREL/TP-500-40566, Dec. 2006.
[18] C. Moné, A. Smith, B. Maples, and M. Hand, "2014 Cost of Wind Energy Review," Nat. Renew. Energy Lab., Golden, CO, USA, Tech. Rep. NREL/TP-6A20-64281, Oct. 2015.
[19] S. Eriksson, H. Bernhoff, "Rotor design for PM generators reflecting the unstable neodymium price," in *Proc. XXth Int. Conf. Elect. Mach.*, Marseille, France, 2012, pp.1419-1423.
[20] J. Carroll, A. McDonald, I. Dinwoodie, D. McMillan, M. Revie, and I. Lazakis, "Availability, operation and maintenance costs of offshore wind turbines with different drive train configurations," *Wind Energ.*,Jul. 2016, [Online]. Available at: http//dx.doi.org/10.1002/we.2011.
[21] *Finite Element Method Magnetics v4.2*. (2016) [Online] Available at: http://www.femm.info/wiki/HomePage
[22] N. A. Bhuiyan and A. McDonald, "Assessment of the Suitability of Ferrite Magnet Excited Synchronous Generators for Offshore Wind Turbines," presented at Eur. Wind Energy Assoc. Offshore Conf., Copenhagen, Denmark, Mar. 10-12, 2015.
[23] S. Eriksson, "Inherent Difference in Saliency for Generators with Different PM Materials," *J. Renew. Energy*, vol. 2014, Nov. 2014, Art. ID. 567896.
[24] J. Pyrhonen, T. Jokinen, V. Hrabovcova, *Design of Rotating Electrical Machines.* Chichester, UK: Wiley, 2009, pp 230-249, 527-529.
[25] W. C. Young and R. G. Budynas, *Roark's Formulas for Stress and Strain*. 7th ed. New York, NY, USA: McGraw-Hill, 2002, pp. 189-192.
[26] P. Jamieson, "Upscaling of Wind Turbine System" in *Innovation in Wind Turbine Design*, 1st ed. Chichester, UK: Wiley, 2011, ch 4, pp 90-94.
[27] J. Carroll, A. McDonald, D. McMillan, T. Stehly, C. Mone, and B. Maples, *"*Cost of energy for offshore wind turbines with different drive train types*,"* presented at Eur. Wind Energy Assoc. Annu. Conf., Paris, France, Nov. 17-20, 2015.
[28] G. Saur, B. Maples, B. Meadows, M. Hand, W. Musial, C. Elkington, J. Clayton, "Offshore Wind Plant Balance-of-Station Cost Drivers and Sensitivities," Nat. Renew. Energy Lab., Golden, CO, USA, Tech. Rep. NREL/PO-5000-56132, Oct. 2012.
[29] MathWorks, Natick, MA, USA. *Global Optimization Toolbox User's guide*. (2016) [Online]. Available at: http://in.mathworks.com/help/pdf_doc/gads/gads_tb.pdf, Accessed on: Mar. 28, 2016.

Alasdair McDonald received the M.Eng. degree in Electrical and Mechanical Engineering from the University of Durham, U.K., in 2004, and a Ph.D. degree in design and modeling of direct drive generators from the University of Edinburgh, UK., in 2008. He is a lecturer in the Wind and Marine Energy Systems Doctoral Training Centre, University of Strathclyde, Glasgow, U.K.

Nurul Azim Bhuiyan received the B.Sc. degree in Electrical and Electronic Engineering from the Ahsanullah University of Science and Technology, Dhaka, Bangladesh in 2007, and a M.Sc. degree in Sustainable Electrical Power from the Brunel University, London, U.K. in 2011. He is currently working toward the Ph.D. degree at the University of Strathclyde, Glasgow, U.K.